Extremely strong thermohaline sources/sinks generated by diagnostic initialization

Peter C. Chu

Naval Ocean Analysis and Prediction Laboratory, Department of Oceanography, Naval Postgraduate School, Monterey, California, USA

Jian Lan

College of Physical and Environmental Oceanography, Ocean University of Qingdao, Qingdao, China

Received 25 October 2002; accepted 27 January 2003; published 29 March 2003.

[1] One difficulty for ocean modeling is the lack of velocity data for specifying the initial condition. Diagnostic initialization is widely used; it integrates the model from known temperature (T_c) and salinity (S_c) and zero velocity fields while holding (T_c, S_c) unchanged. After a period (around 30 days) of the diagnostic run, the velocity field ($\mathbf{V}_c$) is established, and (T_c, S_c, $\mathbf{V}_c$) fields are then treated as the initial conditions for the prognostic numerical modeling. During the diagnostic initialization period, the heat and salt 'source/sink' terms are generated at each time step. Maximum time rates of absolute change of the monthly mean T, S (0.1°/day, 0.1 ppt/day) are taken as the standard measures to identify the strength of the thermohaline 'sources/sinks'. Twenty four times of the standard measures (0.1°/hr, 0.1 ppt/hr) represent strong 'sources/sinks'. Ten times of the strong 'sources/sinks' (1°/hr, 1 ppt/hr) represent extremely strong 'sources/sinks'. The Princeton Ocean Model implemented for the Japan/East Sea is used to demonstrate the existence of extremely strong thermohaline sources and sinks generated by the diagnostic initialization with the annual mean T_c, S_c from the Navy's Global Digital Environmental Model. The effects of extremely strong and spatially nonuniform initial heating/cooling (salting/freshening) rates on thermohaline and velocity fields need to be further investigated. *INDEX TERMS:* 4263 Oceanography: General: Ocean prediction; 4255 Numerical modeling; 4243 Marginal and semienclosed seas; 4520 Oceanography: Physical: Eddies and mesoscale processes; 4528 Fronts and jets. **Citation:** Chu, P., and J. Lan, Extremely strong thermohaline sources/sinks generated by diagnostic initialization, *Geophys. Res. Lett.*, *30*(6), 1341, doi:10.1029/2002GL016525, 2003.

1. Introduction

[2] Ocean modeling aims to integrate hydrodynamic and thermodynamic equations numerically with boundary conditions (lateral and vertical) from initial states of temperature (T), salinity (S), and velocity. Initial T, S fields are relatively easy to obtain, such as using climatological (T_c, S_c) datasets ([e.g., the Navy's Global Digital Environmental Model (GDEM)). However, the initial velocity field is usually not available due to insufficient number of velocity observations. Thus, initialization of the velocity field becomes an important procedure for ocean modeling.

0094-8276/03/2002GL016525$05.00

[3] A widely used model initialization is the diagnostic mode, which integrates the model from known T, S data such as climatological (T_c, S_c) and zero velocity fields, while holding (T_c, S_c) unchanged. After a period (about 30 days) of the diagnostic run, the velocity field ($\mathbf{V}_c$) is established, and (T_c, S_c, $\mathbf{V}_c$) fields are treated as the initial conditions for numerical prognostic modeling. Since initial condition error drastically affects model predictability [*Lorenz*, 1963; *Chu*, 1999], questions arise: Does the diagnostic mode provide ideal initialization? What is the physical process associated with the diagnostic run?

[4] In this study, the Princeton Ocean Model (POM) [*Blumberg and Mellor*, 1987] implemented for the Japan/East Sea (JES) with no surface and lateral forcing is used to investigate the physical outcome of the diagnostic initialization. The GDEM annual mean (T_c, S_c) data with 0.5° × 0.5° resolution are used.

2. Physical Significance of the Diagnostic Mode

[5] Let ($\boldsymbol{V}$, w) be the horizontal and vertical velocity components, and ∇ the horizontal gradient operator. Ocean numerical models are based on the momentum equation

$$\frac{\partial \mathbf{V}}{\partial t} = -\mathbf{V} \bullet \nabla \mathbf{V} - w\frac{\partial \mathbf{V}}{\partial z} - \mathbf{k} \times f\mathbf{V} - \frac{1}{\rho}\nabla p + \frac{\partial}{\partial z}\left(K_M \frac{\partial \mathbf{V}}{\partial z}\right) + \mathbf{H}_{\mathbf{V}}, \tag{1}$$

and the temperature and salinity equations,

$$\frac{\partial T}{\partial t} = -\mathbf{V} \bullet \nabla T - w\frac{\partial T}{\partial z} + \frac{\partial}{\partial z}\left(K_H \frac{\partial T}{\partial z}\right) + H_T, \tag{2}$$

$$\frac{\partial S}{\partial t} = -\mathbf{V} \bullet \nabla S - w\frac{\partial S}{\partial z} + \frac{\partial}{\partial z}\left(K_H \frac{\partial S}{\partial z}\right) + H_S, \tag{3}$$

where f is the Coriolis parameter, ρ the density, p the pressure, and (K_M, K_H) the vertical eddy diffusivity for turbulent mixing of momentum, temperature, and salinity. The terms ($\mathbf{H}_{\mathbf{v}}$, H_T, H_S) represent the subgrid processes causing the local time rate of change in ($\mathbf{V}$, T, S).

[6] The diagnostic mode procedure integrates (1)–(3) from

$$T = T_C,\ S = S_C,\ \mathbf{V} = 0,\ \text{at } t = 0, \tag{4}$$

with T and S unchanged. This procedure is analogous to the process of adding heat and salt source/sink terms (F_T, F_S) in (2) and (3)

$$\frac{\partial T}{\partial t} = -\mathbf{V} \bullet \nabla T - w\frac{\partial T}{\partial z} + \frac{\partial}{\partial z}\left(K_H \frac{\partial T}{\partial z}\right) + H_T + F_T, \tag{5}$$

$$\frac{\partial S}{\partial t} = -\mathbf{V} \bullet \nabla S - w\frac{\partial S}{\partial z} + \frac{\partial}{\partial z}\left(K_H \frac{\partial S}{\partial z}\right) + H_S + F_S, \quad (6)$$

to keep

$$\frac{\partial T}{\partial t} = 0, \ \frac{\partial S}{\partial t} = 0 \quad (7)$$

at the each time step. Comparison of (7) with (5) and (6) leads to

$$F_T \equiv \mathbf{V} \bullet \nabla T + w\frac{\partial T}{\partial z} - \frac{\partial}{\partial z}\left(K_H \frac{\partial T}{\partial z}\right) - H_T, \quad (8)$$

$$F_S \equiv \mathbf{V} \bullet \nabla S + w\frac{\partial S}{\partial z} - \frac{\partial}{\partial z}\left(K_H \frac{\partial S}{\partial z}\right) - H_S. \quad (9)$$

Thus, the heat and salt 'source/sink' terms are generated during the diagnostic initialization at each time step.

3. Measures of 'Source/Sink' Strength

[7] Most diagnostic initialization uses the climatologically monthly (or annual) mean data as the initial T, S conditions. The maximum variability of T, S is estimated by 35°C and 35 ppt. Thus, maximum time rates of absolute change of the monthly mean T, S data (usually taken as initial conditions) are estimated by

$$\left|\frac{\partial T}{\partial t}\right| \le \frac{35°\mathrm{C}}{\mathrm{yr}} \simeq 0.1°\mathrm{C\ day^{-1}}, \quad \left|\frac{\partial S}{\partial t}\right| \le \frac{35\mathrm{ppt}}{\mathrm{yr}} \simeq 0.1\mathrm{ppt\ day^{-1}}, \quad (10)$$

which are taken as the standard measures for 'sources/sinks'. Twenty four times of the standard measures

$$\left|\frac{\partial T}{\partial t}\right|_{Strong} \simeq 0.1°\mathrm{C\ hr^{-1}}, \quad \left|\frac{\partial S}{\partial t}\right|_{Strong} \simeq 0.1\mathrm{ppt\ hr^{-1}}, \quad (11)$$

represent strong 'sources/sinks'. Ten times of the strong 'sources/sinks' $|\partial T/\partial t|_{Strong}$ and $|\partial S/\partial t|_{Strong}$,

$$\left|\frac{\partial T}{\partial t}\right|_{Extra\ Strong} \simeq 1°\mathrm{C\ hr^{-1}}, \quad \left|\frac{\partial S}{\partial t}\right|_{Extra\ Strong} \simeq 1\mathrm{ppt\ hr^{-1}}, \quad (12)$$

represent extremely strong 'sources/sinks'.

4. Diagnostic Initialization for JES Modeling

[8] Question arises: How large are these source/sink terms after the initialization? Are the false 'sources/sinks' bearable for numerical modeling? We use POM implemented for the Japan/East Sea (JES) to evaluate the magnitude of the source/sink terms after the diagnostic initialization.

4.1. Description of JES

[9] JES, covering an area of 10^6 km^2, has steep bottom topography that makes it a unique semi-enclosed ocean basin overlaid by a pronounced monsoon surface wind. It has a maximum depth in excess of 3,700 m, and is isolated from open oceans except for small (narrow and shallow) straits, which connect the JES with the North Pacific through the Tsushima/Korean and Tsugaru Straits and with the Okhotsk Sea through the Soya and Tatar Straits. The smoothed JES bathymetry is shown in Figure 1.

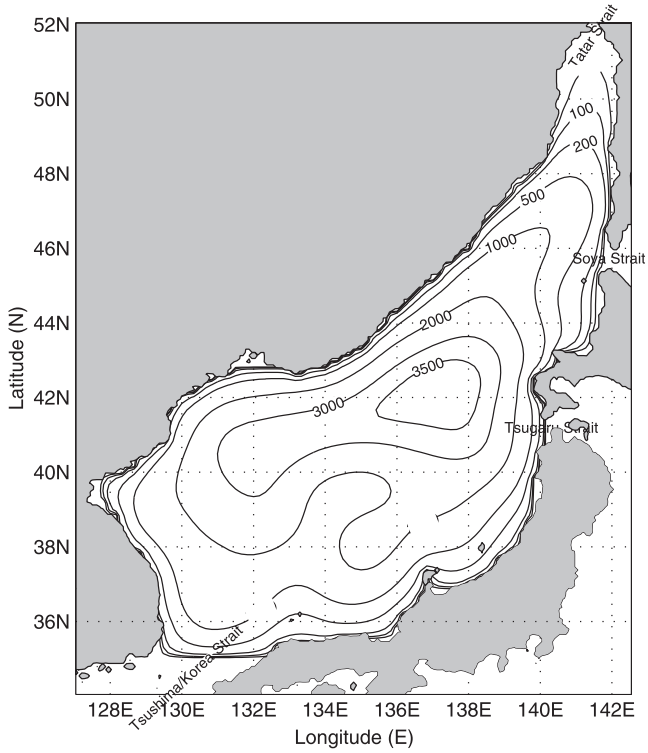

Figure 1. Geography and isobaths showing the bottom topography of the JES model.

[10] The Tsushima Warm Current (TWC), dominating the surface layer, flows in from the Tsushima Strait, and carries warm water from the south up to 40°N where a subpolar front (SPF) forms. Most of the nearly homogeneous water in the deep part of the basin is called the Japan Sea Proper Water [*Moriyasu*, 1972] and is of low temperature and low salinity.

4.2. Model Description

[11] The model contains 94 × 100 horizontally fixed grid points. The horizontal spacing of 10′ latitude and longitude (approximately 11.54 to 15.18 km in the zonal direction and 18.53 km in the latitudinal direction) and 15 vertical nonuniform sigma coordinate levels. The model domain is from 35.0°N to 52°N, and from 127.0°E to 142.5°E. The bottom topography is obtained from the smoothed Naval Oceanographic Office Digital Bathymetry Data Base 5 minute resolution. The horizontal diffusivities are modeled using the Smagorinsky form with the coefficient chosen to be 0.2 for this application. No atmospheric forcing is applied to the model.

[12] Closed lateral boundaries, i.e., the modeled ocean bordered by land, were defined using a free slip condition for velocity and a zero gradient condition for temperature and salinity. No advective or diffusive heat, salt or velocity fluxes occur through these boundaries. At open boundaries, we use the radiative boundary condition with zero volume transport.

4.3. Mode Splitting

[13] For computational efficiency, the mode splitting technique [*Blumberg and Mellor*, 1987] is applied with a barotropic time step of 24 seconds, based on the Courant-

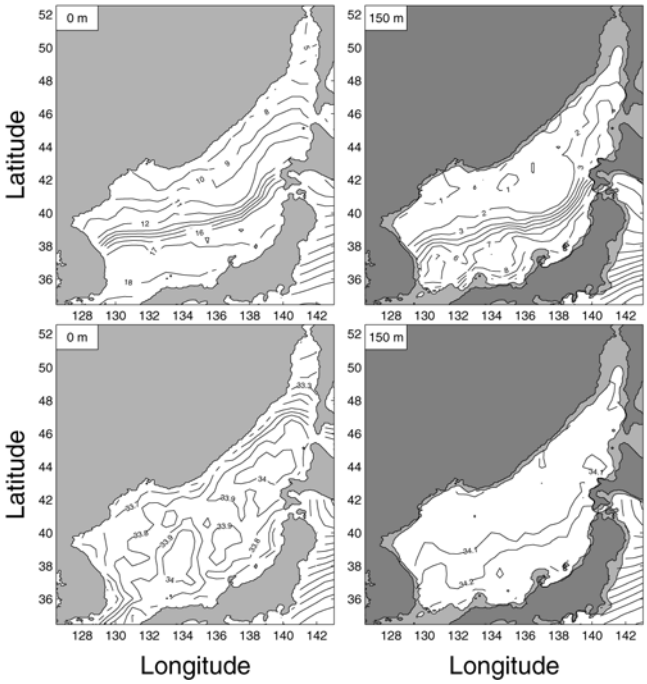

Figure 2. GDEM annual mean (a) temperature and (b) salinity at various depths.

Friederichs-Levy (CFL) computational stability condition and the external wave speed; and a baroclinic time step of 720 seconds, based on the CFL condition and the internal wave speed.

4.4. Climatological T, S Data

[14] The annual mean GDEM *T*, *S* data are used for the study [*Chu et al.*, 2001]. Here, the fields at the surface and 150 m depth are presented. The depth of 150 m corresponds to the permanent thermocline and the middle level of the Japan Sea Intermediate Water. Below the depth of 150 m, the water mass is quite uniform. Non-uniform heat/salt source and sink terms might cause abrupt thermohaline change.

[15] The climatological mean temperature field at two depths (0, 150 m) clearly shows the existence of the SPF with the position around 38°N in the west and near 42°N in the east (Figures 2a and 2b). The temperature is more than 6°C higher south of SPF than north of SPF at 0 and 150 m. The climatological mean salinity field at the surface (Figure 2c) clearly shows that the saline Kuroshio water (>34.2 ppt) enters the JES from the Tsushima/Korean Strait into the JES and forms two permanent salty centers with the salinity higher than 34.0 ppt, located north of SPF (west of the Hokkaido Island) and south of SPF at 37°–40°N, 132°–136°E.

4.5. Diagnostic Mode

[16] The POM was integrated in the diagnostic mode with all three components of velocity (u, v, w) initially set to zero, and with temperature and salinity specified by interpolating GDEM annual mean data to each model grid point. F_T and F_S are obtained at each time step. The diagnostic model was integrated for 60 days, 30 days were sufficient for the volume-mean model kinetic energy to reach quasi-steady state under the imposed conditions (Figure 3). The thermohaline source/sink terms (F_T, F_S) generated by the diagnostic initialization on day-30 and

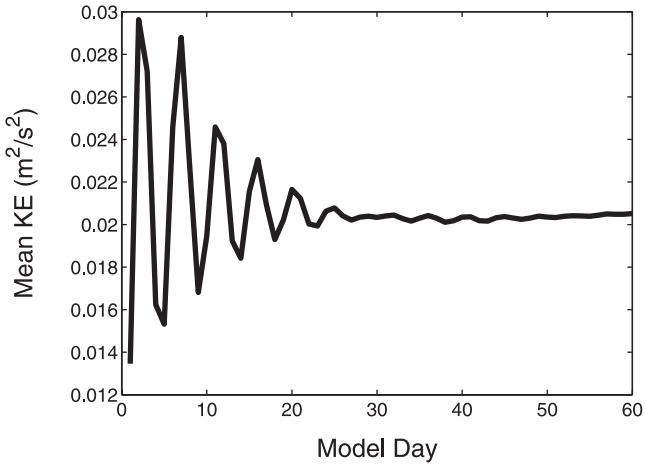

Figure 3. Temporal variation of total kinetic energy. Note that the quasi-steady state is reached after 30 day's integration.

day-60 are used to identify their magnitudes and sensitivity to the integration period.

5. Source/Sink Terms in Diagnostic Initialization

5.1. Heat Sources/Sinks

[17] Horizontal distributions of $\rho c_p F_T$ (unit: W m^{-3}) on day-30 (Figure 4) at the four σ levels (0, −0.143, −0.5, and −0.929) show extremely strong heat sources/sinks generated by the diagnostic initialization. For $\rho c_p F_T$ = 1000 W m^{-3}, the time rate of absolute temperature change F_T = 0.84°C hr^{-1}. The sources/sinks have various scales and strengths. They reveal small- to meso-scale patterns in most areas except a large-scale pattern near the bottom (σ = −0.929). The strength of the source/sink increases with depth from the surface to subsurface. The extremely strong source reaching 5164W m^{-3} (corresponding to F_T = 4.34°C

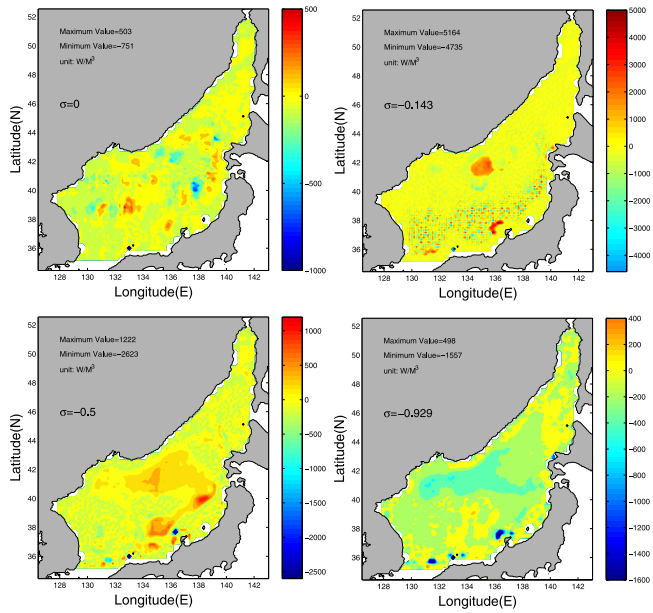

Figure 4. Horizontal distribution of $\rho c_p F_t$ (unit: W m^{-3}) on day-30 at σ levels of: (a) 0, (b) −0.143, (c) −0.5, and (d) −0.929.

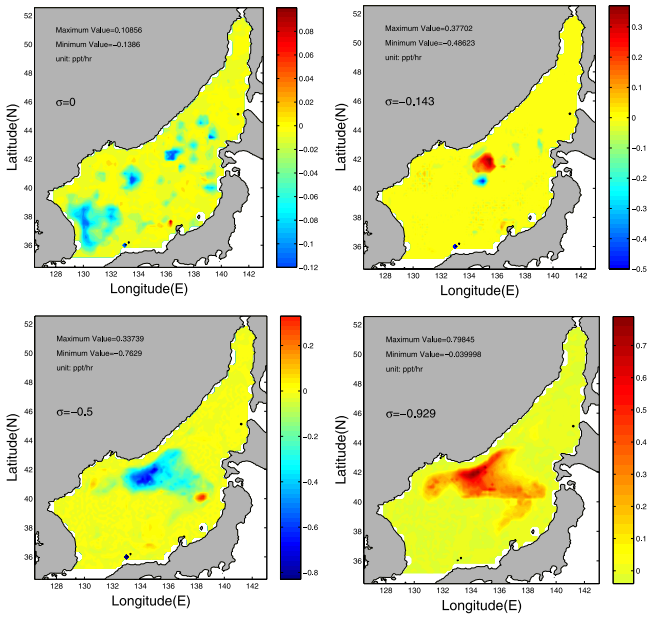

Figure 5. Horizontal distribution of F_S (unit: ppt s^{-1}) on day−30 at σ levels of: (a) 0, (b) −0.143, (c) −0.5, and (d) −0.929.

hr^{-1}) and the extremely strong sink reaching −4735 Wm^{-3} (corresponding to $F_T = -3.98°C\ hr^{-1}$), and decreases with depth below the subsurface. Near the bottom, the JES basin is dominated by cooling with the maximum sink strength −1557 Wm^{-3} (corresponding to $F_T = -1.31°C\ hr^{-1}$). From the subsurface to the bottom, the source/sink terms have some organized pattern near the SPF. At the subsurface, a dipole pattern occurs between 133°−136°E with strong source strength approximate 2000 W m^{-3} (corresponding to $F_T = 1.68°C\ hr^{-1}$) north of the SPF and cooling rate (∼ −2000 W m^{-3}) south of the SPF. Near the bottom, a large cooling area with the cooling rate of 750 Wm^{-3} occurs north of the SPF.

5.2. Salt Sources/Sinks

[18] Horizontal distributions of F_s (unit: ppt m^{-3}) on day-30 (Figure 5) at the four σ levels (0, −0.143, −0.5, and −0.929) show near-extremely strong salinity sources/sinks generated by the diagnostic initialization. These sources/sinks have various scales and strengths. They reveal small- to meso-scale patterns in most areas but a large-scale pattern in the southern JES near Tsushima/Korean Strait at the surface and north of the SPF at the mid-level and bottom. The strength of the source/sink increases with depth from the surface to the bottom. The maximum salinity source (sink) is found 0.80 ppt hr^{-1} (−0.76 ppt hr^{-1}) at σ = −0.929 (σ = −0.5).

6. Discussion

[19] When the prognostic integration starts, the source/sink terms F_T and F_S are removed from (5) and (6). Extremely strong and spatially nonuniform initial heating/cooling (salting/freshening) rates are introduced in the ocean models and cause drastic changes in thermohaline and velocity fields initially (after the diagnostic run) especially in the deep layer below the thermocline and halocline. Note that the problem is caused by the diagnostic initialization only, nothing to do with the ocean model itself.

[20] In the diagnostic initialization, the source/sink terms drive the velocity through the pressure gradient force (see equation (1)). The pressure gradient error leads to errors in the initialized velocity field. Different models (*z*-level, σ-level, and *s*-level) have different pressure gradient errors, which in turns generate different initial velocity fields. Besides, the diagnostic process (spin up/down) largely depends on the diffusion. The spin down scale of 30 days is the state of balance between the pressure gradient force (not change with time) and other terms in equation (1) such as the diffusion term that depends not only on the velocity field, but also on the model parameters. Thus, the diagnostic initialization depends on model type and model parameters.

[21] If the diagnostic initialization continues to be used, it is urgent to study the following problems: Does this artificial initial heating/cooling (salting/freshening) induce false chaotic motion in ocean models? How long does the ocean model need to be adjusted? Does the spin-up of the prognostic run have the capability to diminish this initial effect?

[22] If the monthly mean T_c, S_c data are used as the initial conditions, the initial heating (or cooling) and salting (or freshening) rates should not be greater than the standard measures (10) everywhere in the domain. If they reach the levels of strong 'sources/sinks' ($|\partial T/\partial t|_{Strong}$ and $|\partial S/\partial t|_{Strong}$), the calculated ($T_c$, S_c, $\mathbf{V}_c$) fields after diagnostic initialization are abnormal. If they reach the levels of extra strong 'sources/sinks' ($|\partial T/\partial t|_{ExtraStrong}$ and $|\partial S/\partial t|_{ExtraStrong}$), the calculated ($T_c$, S_c, $\mathbf{V}_c$) fields cannot be used. Thus, development of a check-up algorithm on strength of the initial source and sink is urgent.

[23] **Acknowledgments.** The authors would like to thank George Mellor and Tal Ezer of Princeton University for most kindly providing a copy of POM code. The Office of Naval Research and Naval Oceanographic Office sponsored this research.

References

Blumberg, A., and G. Mellor, A description of a three dimensional coastal ocean circulation model, in *Three-Dimensional Coastal Ocean Models, Coastal Estuarine Ser.*, vol. 4, edited by N. S. Heaps, pp. 1–16, AGU, Washington, D. C., 1987.

Chu, P. C., Two kinds of predictability in Lorenz system, *J. Atmos. Sci.*, *56*, 1427–1432, 1999.

Chu, P. C., J. Lan, and C. W. Fan, Japan Sea circulation and thermohaline structure, part 1, Climatology, *J. Phys. Oceanogr.*, *31*, 244–271, 2001.

Lorenz, E. N., Deterministic nonperiodic flow, *J. Atmos. Sci.*, *20*, 130–141, 1963.

Moriyasu, S., The Tsushima current, *Kuroshio, Its Physical Aspects*, edited by H. Stommel and K. Yoshida, pp. 353–369, Univ. of Tokyo Press, Tokyo, 1972.

P. C. Chu, Naval Ocean Analysis and Prediction Laboratory, Department of Oceanography, Naval Postgraduate School, 833 Dyer Road, Room 328, Monterey, CA 93943, USA. (pcchu@nps.navy.mil)

J. Lan, College of Physical and Environmental Oceanography, Ocean University of Qingdao, Qingdao 266003, China. (lanjian@lib.ouc.edu.cn)